11218-2-T = RL-2212

011218-2-T

THE UNIVERSITY OF MICHIGAN

COLLEGE OF ENGINEERING

DEPARTMENT OF ELECTRICAL AND COMPUTER ENGINEERING

Radiation Laboratory

APPLICATION OF THE LARGE GRADIENT VOR ANTENNA

By

Dipak L. Sengupta and Philip Chan

15 December 1972

Interim Engineering Report No. 2

Contract No. DOT-FA72WA-2882
Project No. WA5R-1-0526/N113-739.0

Contract Monitor: Mr. Sterling R. Anderson, RD 331

Prepared For:

FEDERAL AVIATION ADMINISTRATION
800 Independence Avenue, S. W.
Washington, D.C. 20591

2216 Space Research Building
2455 Hayward Street
Ann Arbor, Michigan
48105

TABLE OF CONTENTS

I

INTRODUCTION

This is the second Interim Report on Contract No. DOT-FA72WA-2882, "Application of the Large Gradient VOR Antenna," and covers the period 1 September to 30 November, 1972.

The present report investigates theoretically the radiation pattern of Scanwell antennas located in free space and above a perfectly conducting infinite planar ground. The organization of the report and some of the notations used are similar to our Interim Engineering Report No. 1 (Sengupta and Chan, 1972).

II

THE SCANWELL ANTENNA

The Scanwell antenna is a large gradient VOR antenna developed by the Scanwell Laboratories. It consists of a linear array of five elements or bays. Each bay consists of a standard 4-loop VOR array (Anderson et al, 1953). Figure 1 shows schematically the array geometry. The direction of the z-axis will be referred to as the vertical direction. The numbering of the array elements is as shown in Fig. 1. The position of the nth element with respect to the origin is denoted by d_n. Note that d_n is positive for elements above the x-axis and negative for elements below the x-axis. As can be seen from Figure 1, the array is non-uniformly spaced and excited. However, the spacing of the antenna elements are symmetrical with respect to the x-axis.

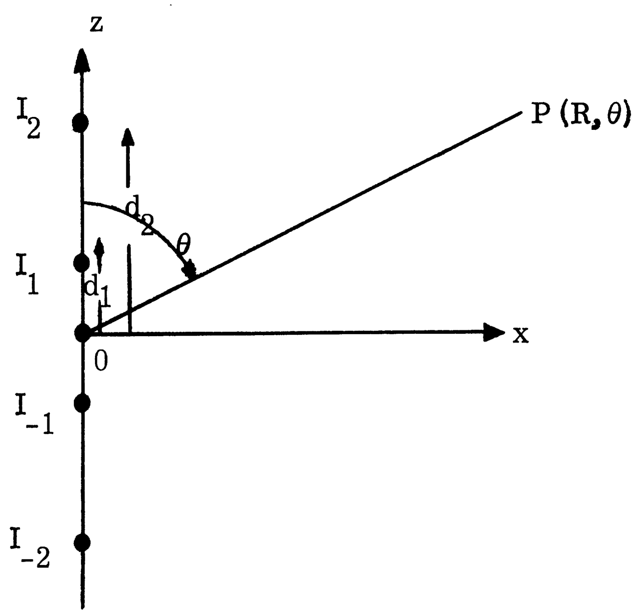

FIGURE 1: Schematic representation of the Scanwell antenna.

The Scanwell laboratories optimized the antenna parameters I_n $(= |I_n| e^{i\alpha_n})$, d_n such that the free space pattern of the antenna in the x-z plane produces maximum field gradient (α_g) at the horizon. The optimum parameters of the antenna under such conditions are such that the following conditions hold:

$$\left.\begin{array}{l} |I_n| = |I_{-n}| \\ \\ \alpha_n = -\alpha_{-n}, \\ \quad \text{where } \alpha_n \text{ is the angle of } I_n, \\ \\ d_n = |d_{-n}| \end{array}\right\} \tag{1}$$

It is now assumed that each element or bay has a $\sin\theta$ - type of pattern in the z-x plane. Thus, the free space vertical plane complex pattern of the antenna may be written as follows:

$$S(\theta) = \sin\theta \left[|I_0| + 2 \sum_{n=1}^{2} |I_n| \cos(kd_n \cos\theta - \alpha_n) \right] \tag{2}$$

The fundamental approximation made in Equation (2) is that the element pattern, i.e., the pattern of the 4-loop VOR array is $\sin\theta$ - type in the x- z plane and that it is the same in both carrier and side-band modes. Because of this Equation (2) indicates that the antenna has the same pattern in the carrier and side band mode of operation. As discussed earlier (Sengupta and Chan, 1972), the slightly different nature of the side-band and carrier mode patterns can be taken into account by using the proper element pattern in Equation (2).

III

FREE SPACE PATTERNS

In this section we give the free space vertical plane radiation patterns of the Scanwell antenna. Figure 2 shows the free space pattern of the optimum Scanwell antenna. The excitation coefficients of the optimum antenna, as obtained by the Scanwell Laboratories, are as follows:

$$|I_0| = 1, \quad \alpha_0 = 0$$
$$|I_1| = 0.62, \quad \alpha_1 = 96^\circ.3$$
$$|I_2| = 0.19, \quad \alpha_2 = 108^\circ.9 \ .$$

The element spacings in the optimum antenna are $d_1 = \lambda/2$, $d_2 = 3\lambda/2$ where λ is the operating wavelength. The field gradient obtained for the optimum antenna is $\alpha_g \simeq 16$ dB/6°.

We have also obtained free space patterns of the antenna for slightly different excitations but with the same element spacings. The following table gives the excitations and the corresponding field gradients obtained:

$\lvert I_0\rvert$	$\lvert I_1\rvert$	$\lvert I_2\rvert$	α_0	α_1	α_2	α_g
1	0.55	0.15	0	$96^\circ.3$	$108^\circ.9$	10.20 dB/6°
1	0.50	0.10	0	$96^\circ.3$	108.9	6.74 dB/6°
1	0.62	0	0	96.3	0	5.27 dB/6°
1	0.4	0.10	0	$96^\circ.3$	108.9	4.98 dB/6°

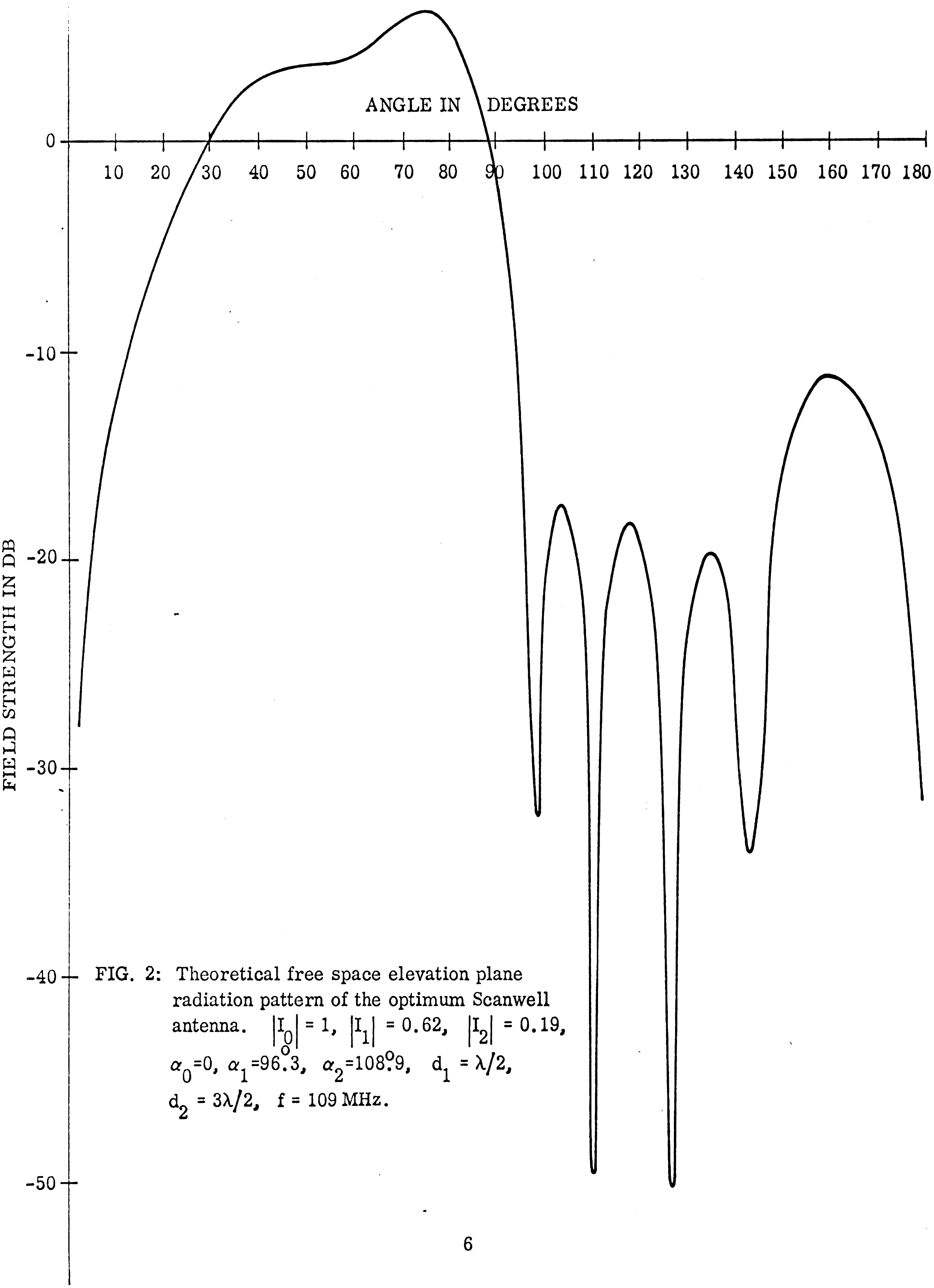

FIG. 2: Theoretical free space elevation plane radiation pattern of the optimum Scanwell antenna. $|I_0| = 1$, $|I_1| = 0.62$, $|I_2| = 0.19$, $\alpha_0=0$, $\alpha_1=96^{\circ}.3$, $\alpha_2=108^{\circ}.9$, $d_1 = \lambda/2$, $d_2 = 3\lambda/2$, f = 109 MHz.

Figure 3 shows the complete patterns of the antenna for different excitations. It can be seen from Figure 3 that for the variation of the excitation used here, the main beam of the pattern is not affected appreciably. However, the field gradient as well as the minor lobe details are affected considerably by the change in the excitations. It should be noted that the standard 4-loop array pattern has a field gradient of about $3dB/6^{o}$ in both carrier and side-band mode of operation.

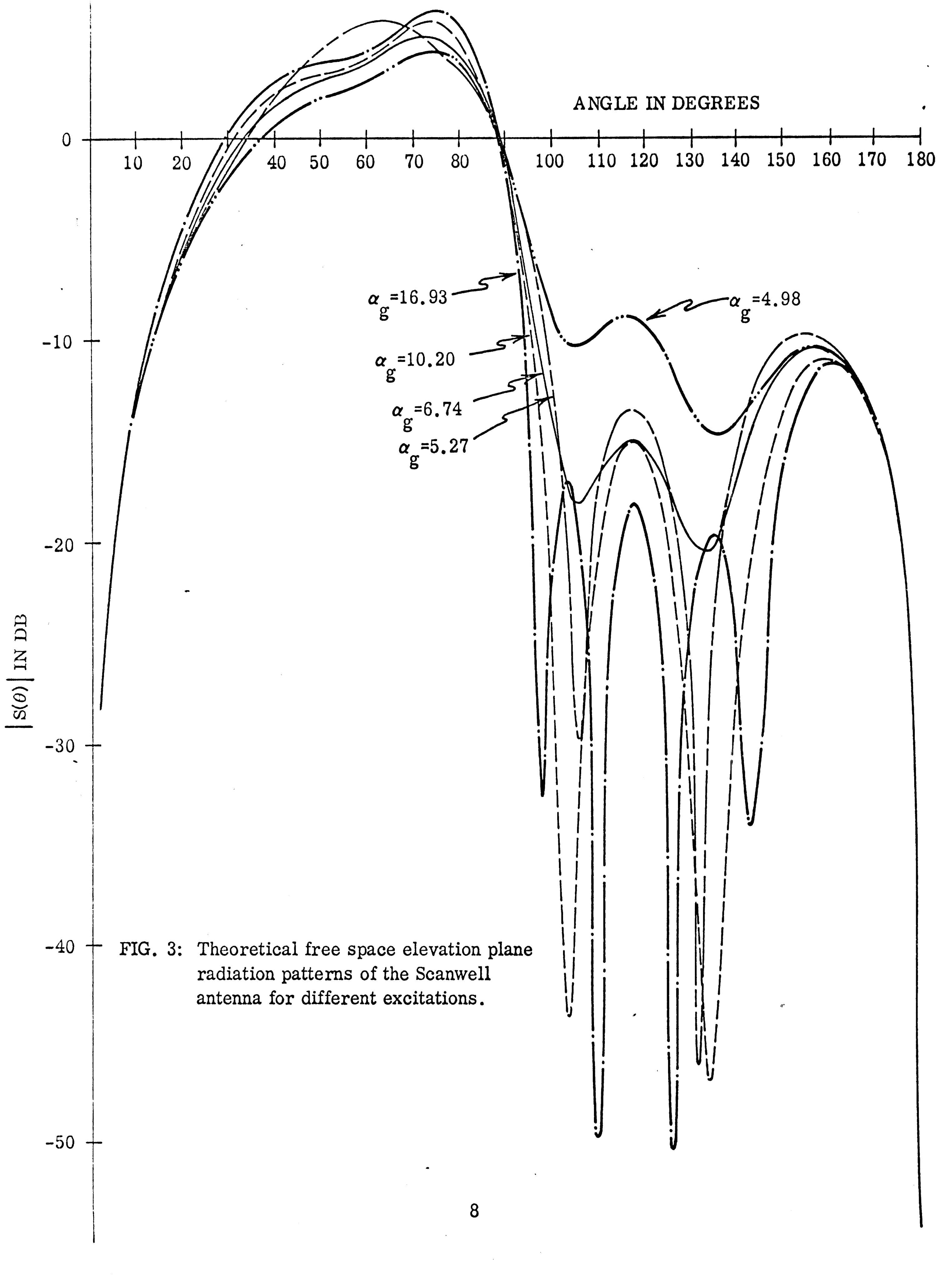

FIG. 3: Theoretical free space elevation plane radiation patterns of the Scanwell antenna for different excitations.

IV

SCANWELL ANTENNAS ABOVE GROUND

In this section we discuss the patterns of Scanwell antennas located above a perfectly conducting infinite planar ground. The far field patterns are obtained by using the following expression:

$$S_T(\theta) = e^{-ikz\cos\theta} S(\theta) - e^{ikz\cos\theta} S(\pi-\theta) , \tag{3}$$

$$0 \le \theta \le \pi/2 ,$$

where $S(\theta)$ is given by Equation (2) and z is the height of the center element $(n = 0)$ above ground.

Complete patterns for the antenna have been computed by using Equation (3) for selected values of Z_1 in the range $0 \le Z_1 \le 500'$. During this part of the computation the patterns have been calculated in the range $0 \le \theta \le \pi/2$ at 1^o intervals. Some of the patterns for selected values of Z_1 are shown in Figures (4a-4d). Figures (5a-e) give the patterns of the same antenna in the range $80^o \le \theta \le 90^o$ and for different values of the heights. These patterns have been computed at 0.1^o intervals for sufficient accuracy. Figure 6 shows the positions of the few minima above horizon $(\theta = \pi/2)$ as functions of the antenna height. Notice that the position of a minimum is expressed in angles above the horizon, i.e., above 90^o. The curves given in Figure 6 are self explanatory. The index n in Figure 6 denotes the number of the minimum above the horizon; $n = 1$ is the minimum in the pattern closest to the horizon. Figure 7 shows the depths of the first few minima as a function of the antenna height. In general it can be said that the depths of a minimum increases continuously with Z_1. For a given Z_1, the minimum nearest to the horizon is deepest and the depth decreases with the order of the minimum. Figure 8 shows the variation of the filling factor versus height for the first few minima in the pattern obtained by using the optimum antenna as compared with those obtained with a standard VOR antenna when the two antennas are located at the same height. Figure 8 indicates that for each minimum initially the filling factor increases rapdily with height and then it approaches a constant value of about 10dB.

Figures 9, 10 and 11 show respectively the position of the minima, depths of the minima and the fillings factors as functions of height for the Scanwell antenna with $\alpha_g = 10$ dB/6^o. The corresponding curves for $\alpha_g = 6.74$ dB/6^o are given in Figures 12 - 14 and those for $\alpha_g = 4.98$dB/6^o are given in Figures 15 - 17.

In general, for a given Z_1, the depth of a minimum (say $n = 1$) increases as α_g decreases. This is as it should be. The positions of the minima appears to be independent of α_g for $Z_1 \geq 100'$. For $Z_1 < 100'$, the positions of the minima increase as the gradient decreases. Most importantly, the saturation value of the filling factor decreases as the field gradient value α_g decreases.

The depth of the first minimum and the filling factor of the first minimum are shown in Figure 18 as functions of α_g for the particular height $Z_1 = 200'$.

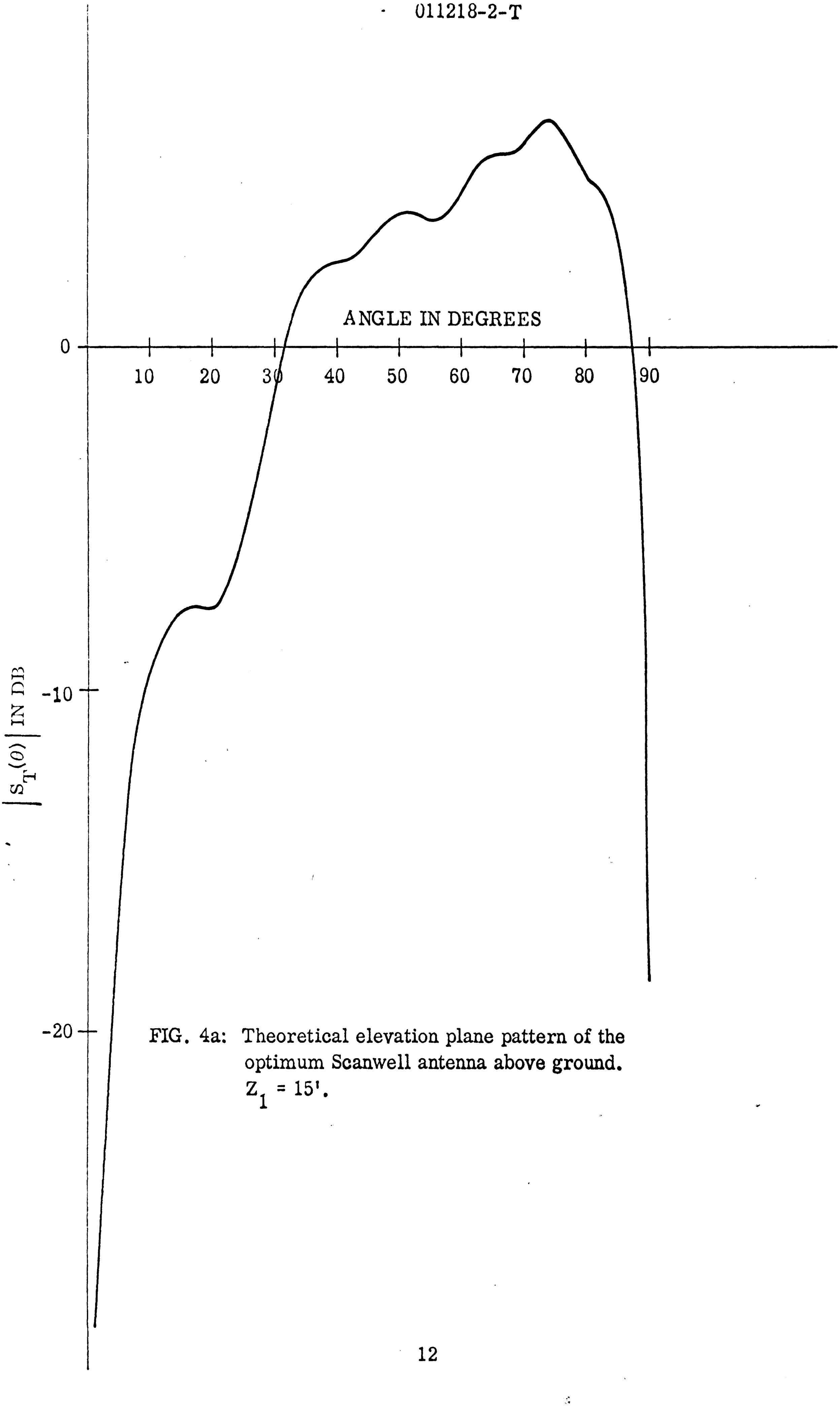

FIG. 4a: Theoretical elevation plane pattern of the optimum Scanwell antenna above ground. $Z_1 = 15'$.

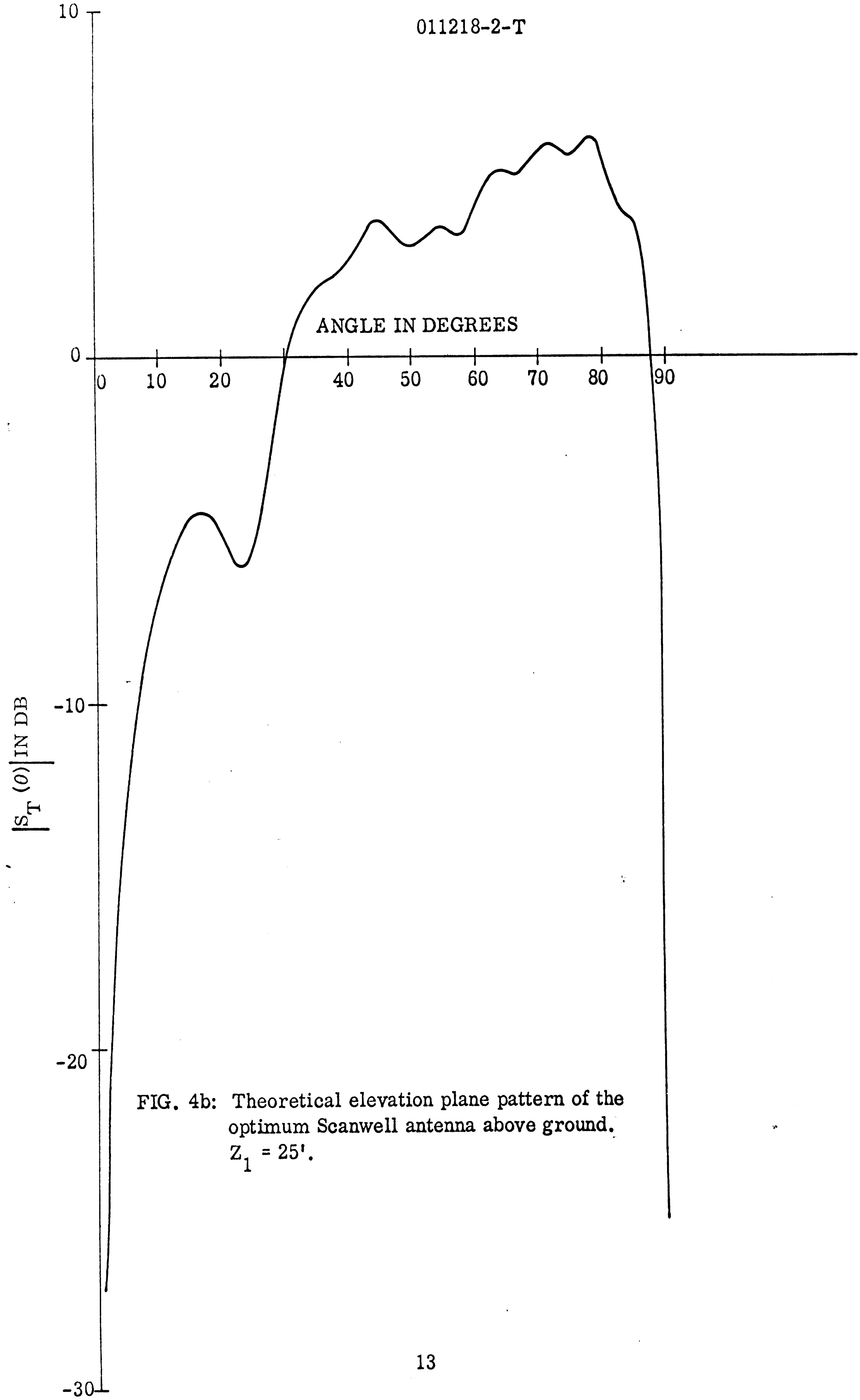

FIG. 4b: Theoretical elevation plane pattern of the optimum Scanwell antenna above ground. $Z_1 = 25'$.

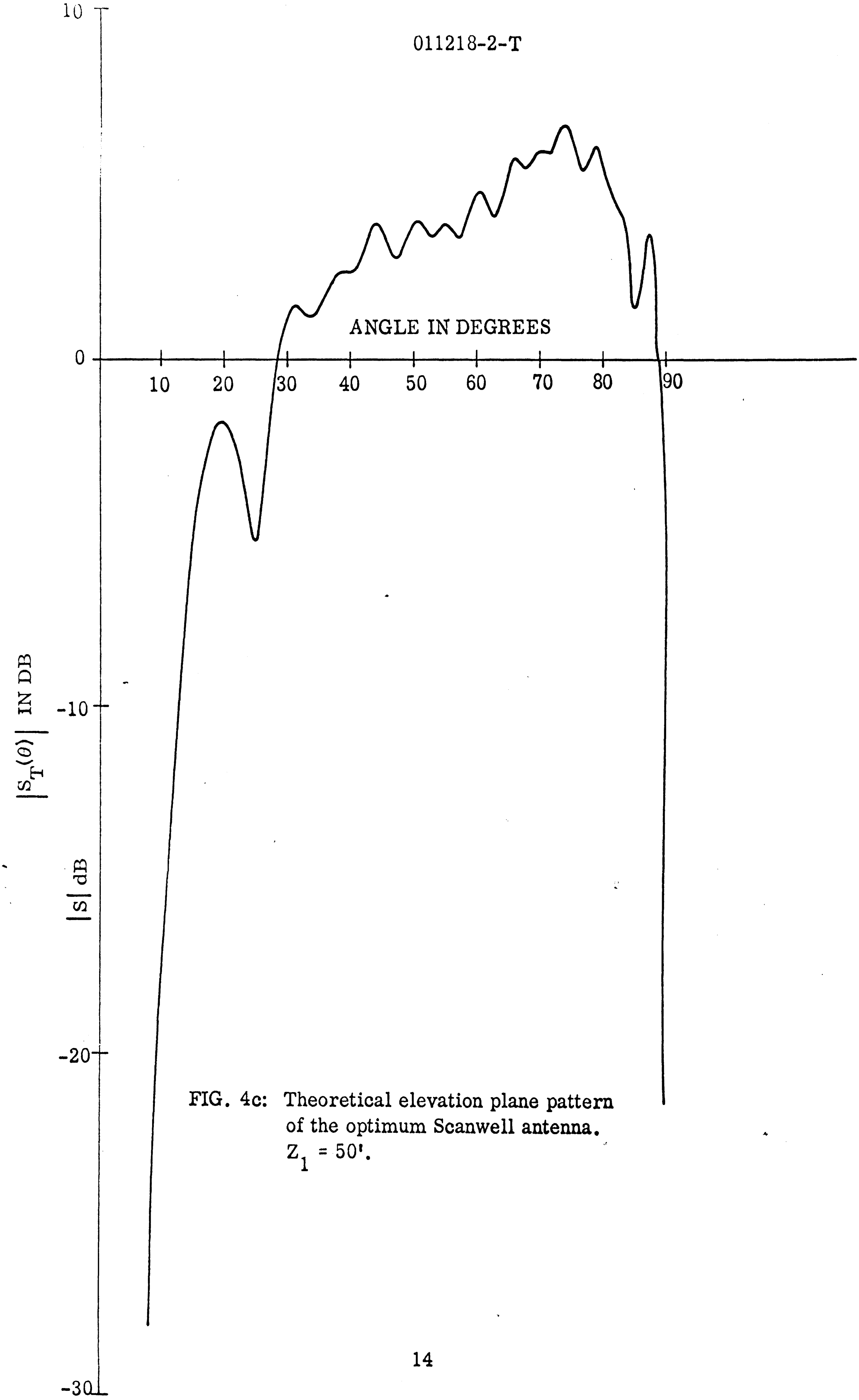

FIG. 4c: Theoretical elevation plane pattern of the optimum Scanwell antenna. $Z_1 = 50'$.

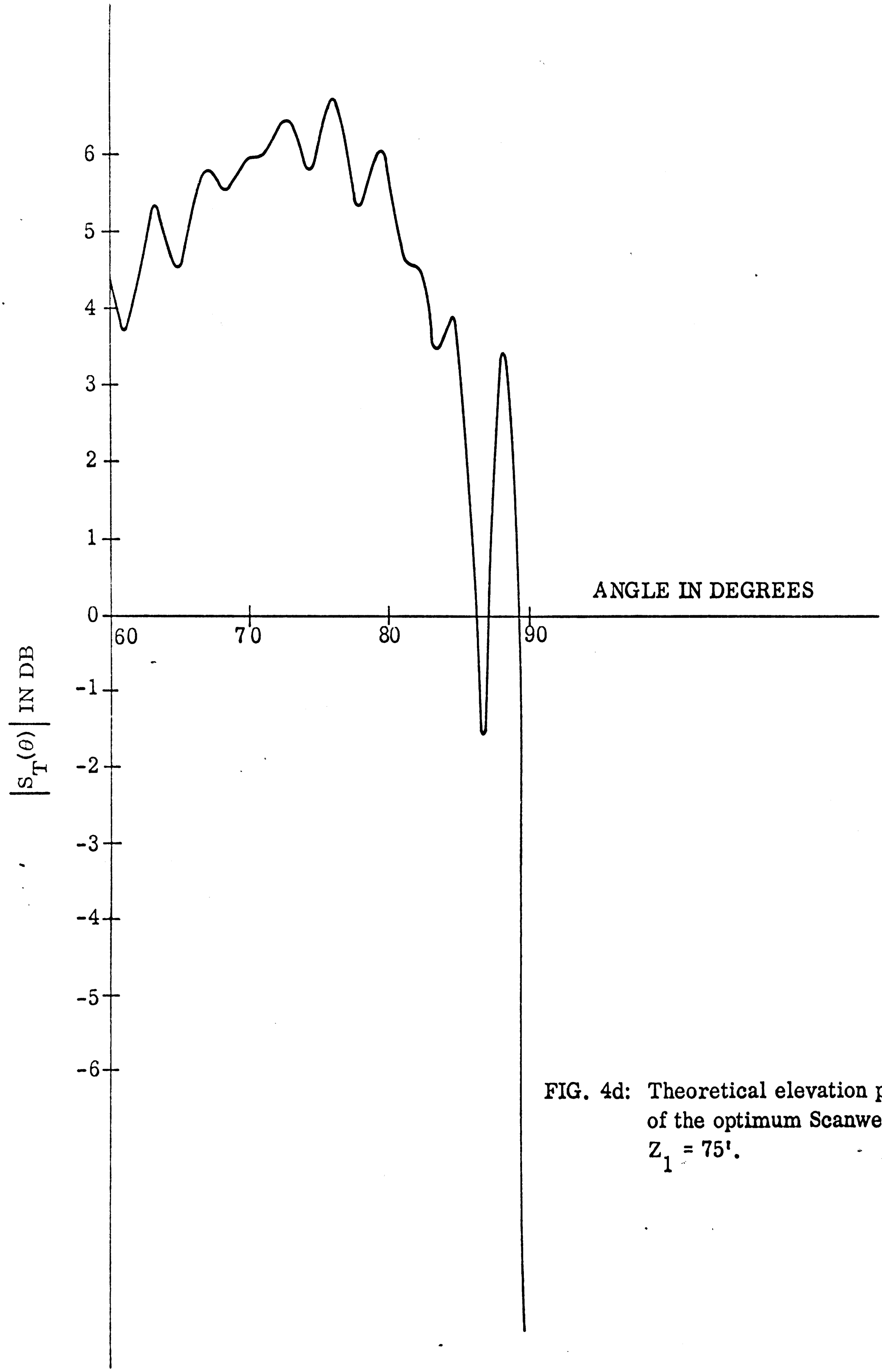

FIG. 4d: Theoretical elevation plane pattern of the optimum Scanwell antenna. $Z_1 = 75'$.

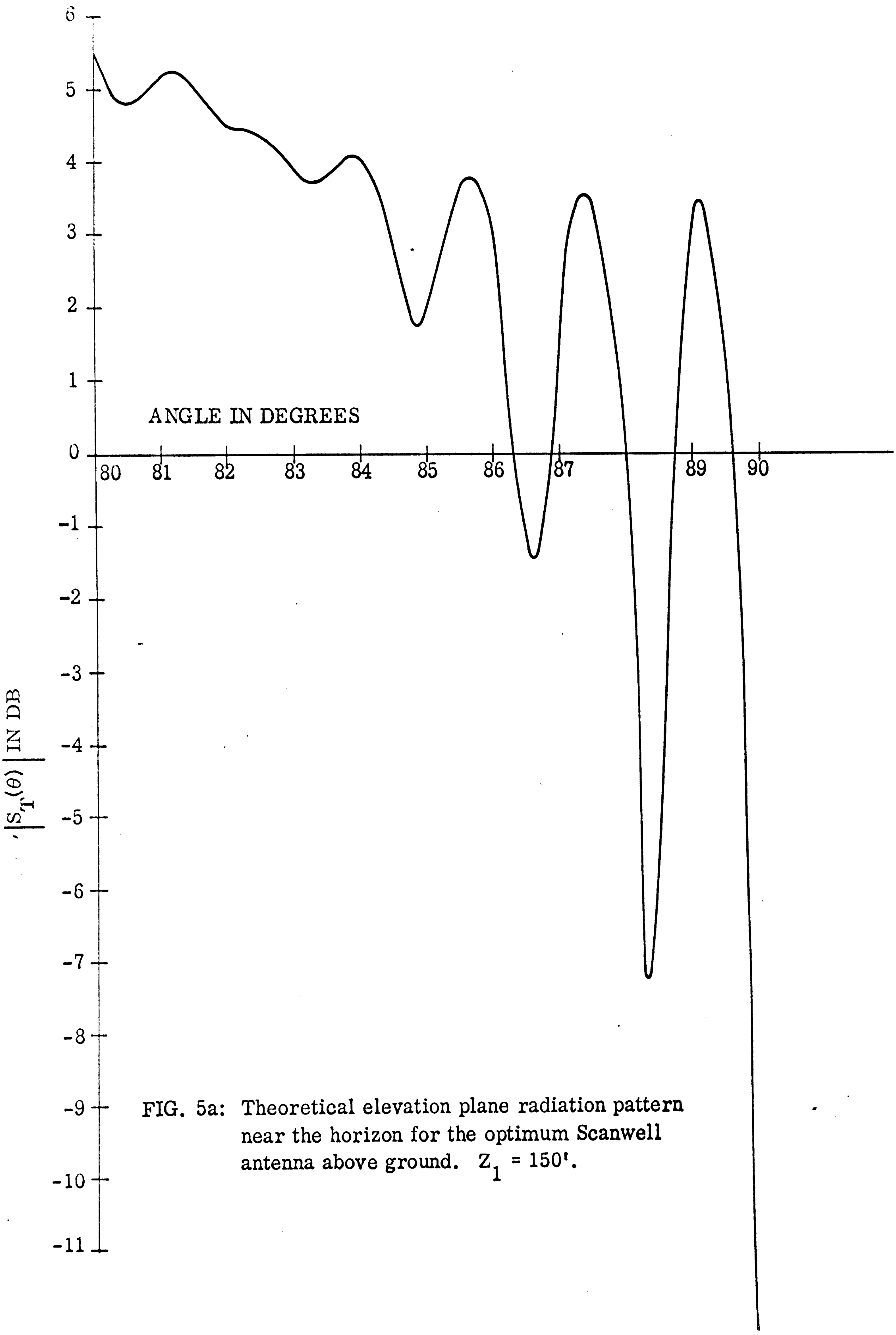

FIG. 5a: Theoretical elevation plane radiation pattern near the horizon for the optimum Scanwell antenna above ground. $Z_1 = 150'$.

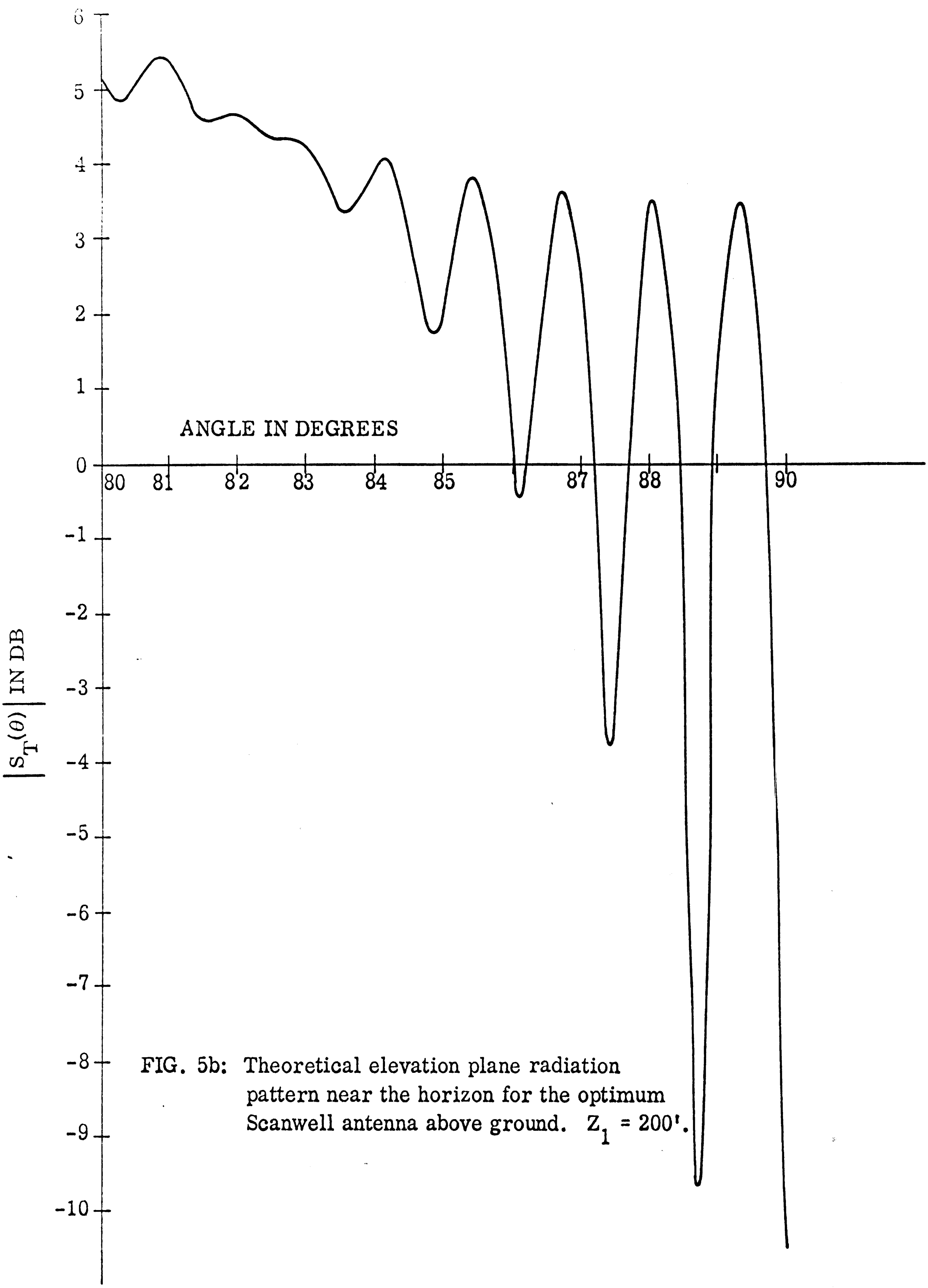

FIG. 5b: Theoretical elevation plane radiation pattern near the horizon for the optimum Scanwell antenna above ground. $Z_1 = 200'$.

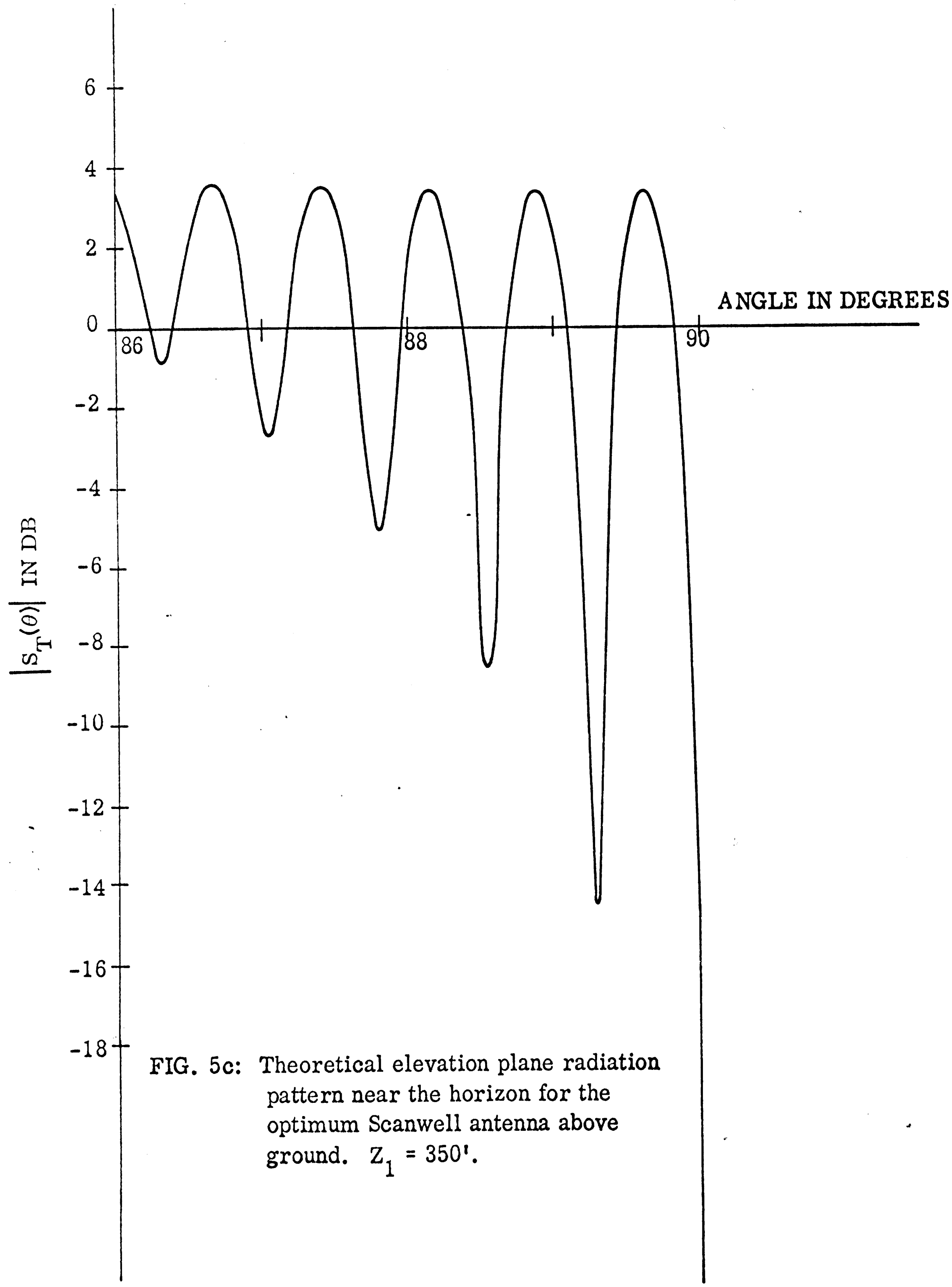

FIG. 5c: Theoretical elevation plane radiation pattern near the horizon for the optimum Scanwell antenna above ground. Z_1 = 350'.

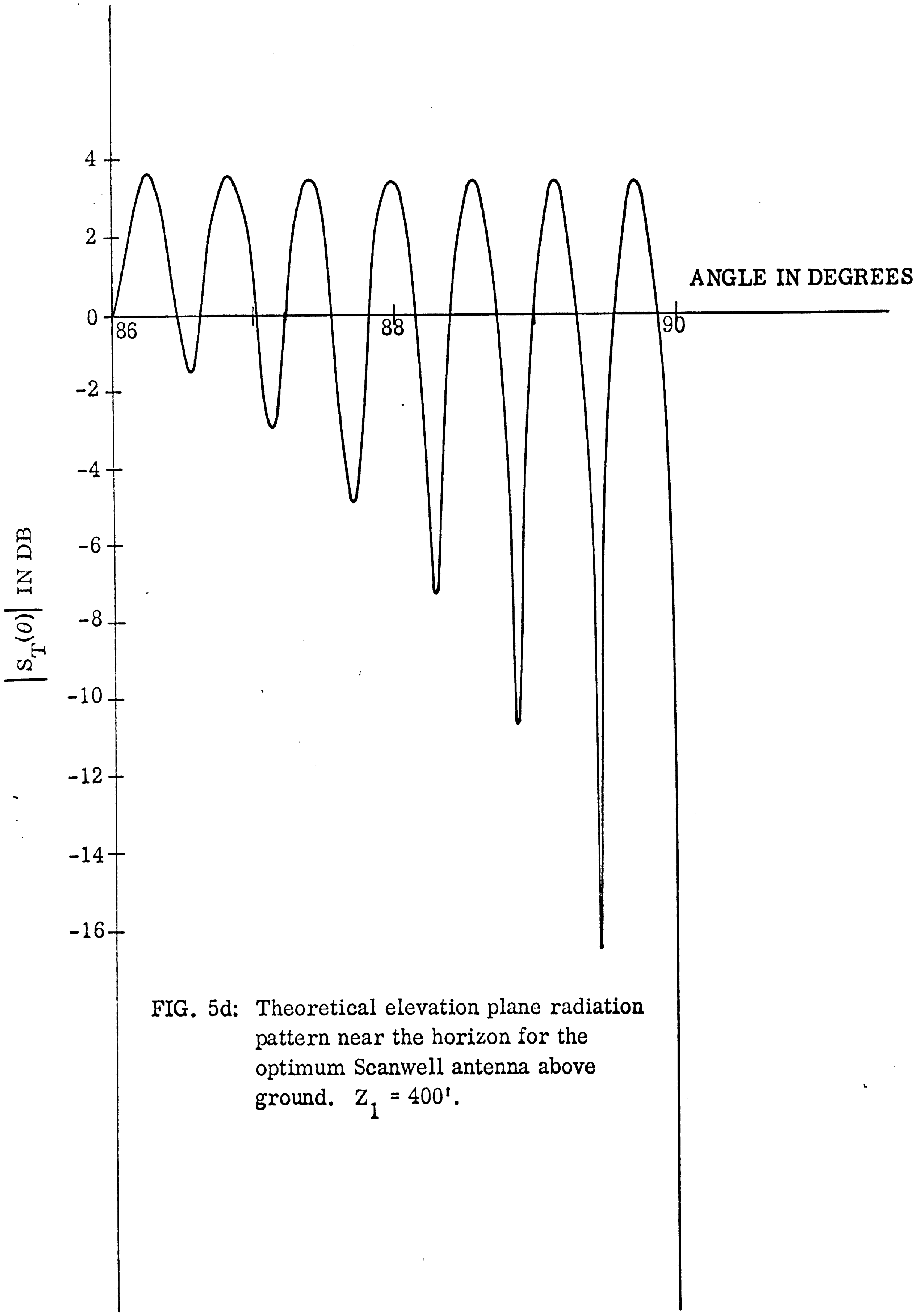

FIG. 5d: Theoretical elevation plane radiation pattern near the horizon for the optimum Scanwell antenna above ground. Z_1 = 400'.

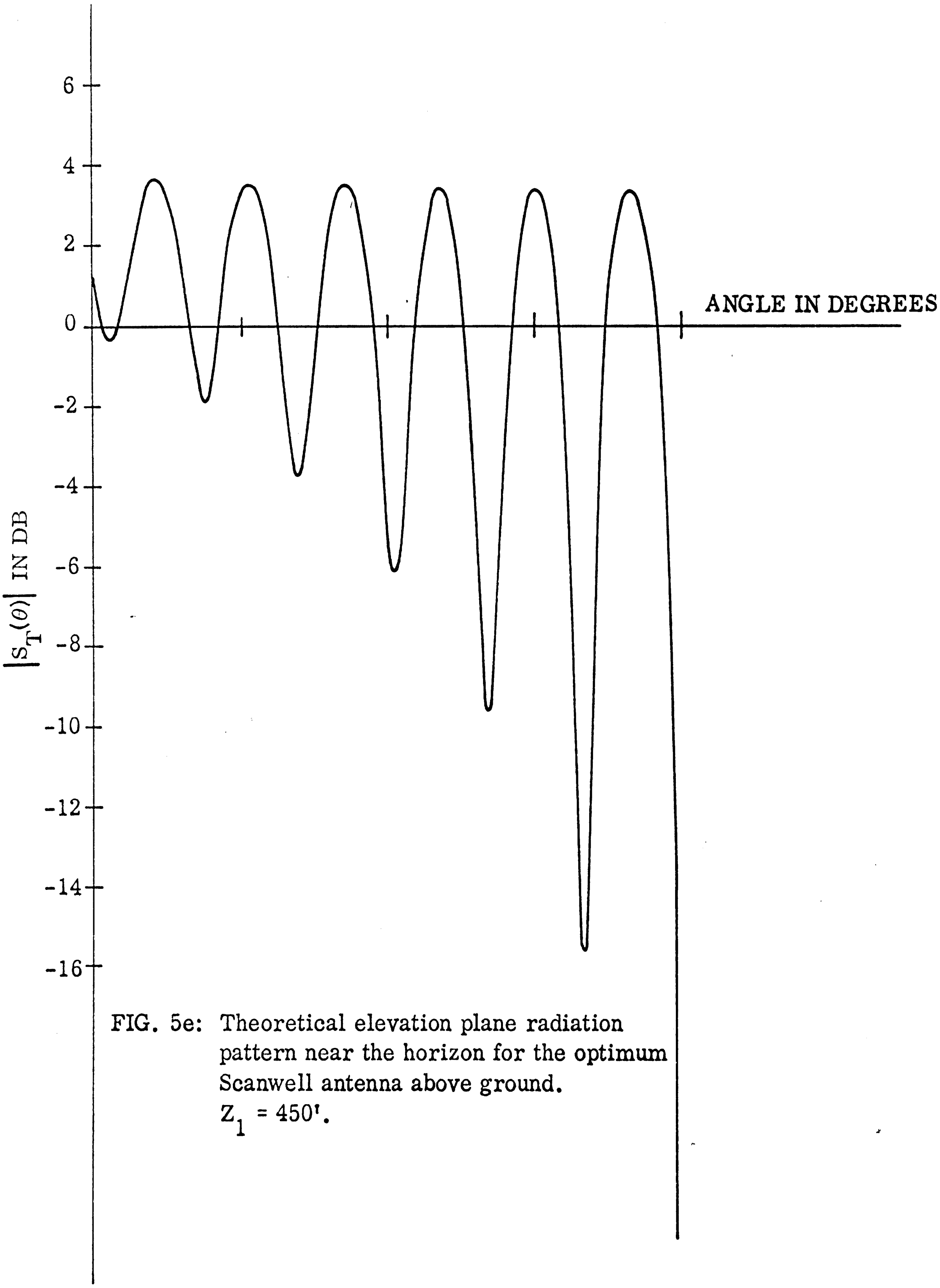

FIG. 5e: Theoretical elevation plane radiation pattern near the horizon for the optimum Scanwell antenna above ground. Z_1 = 450'.

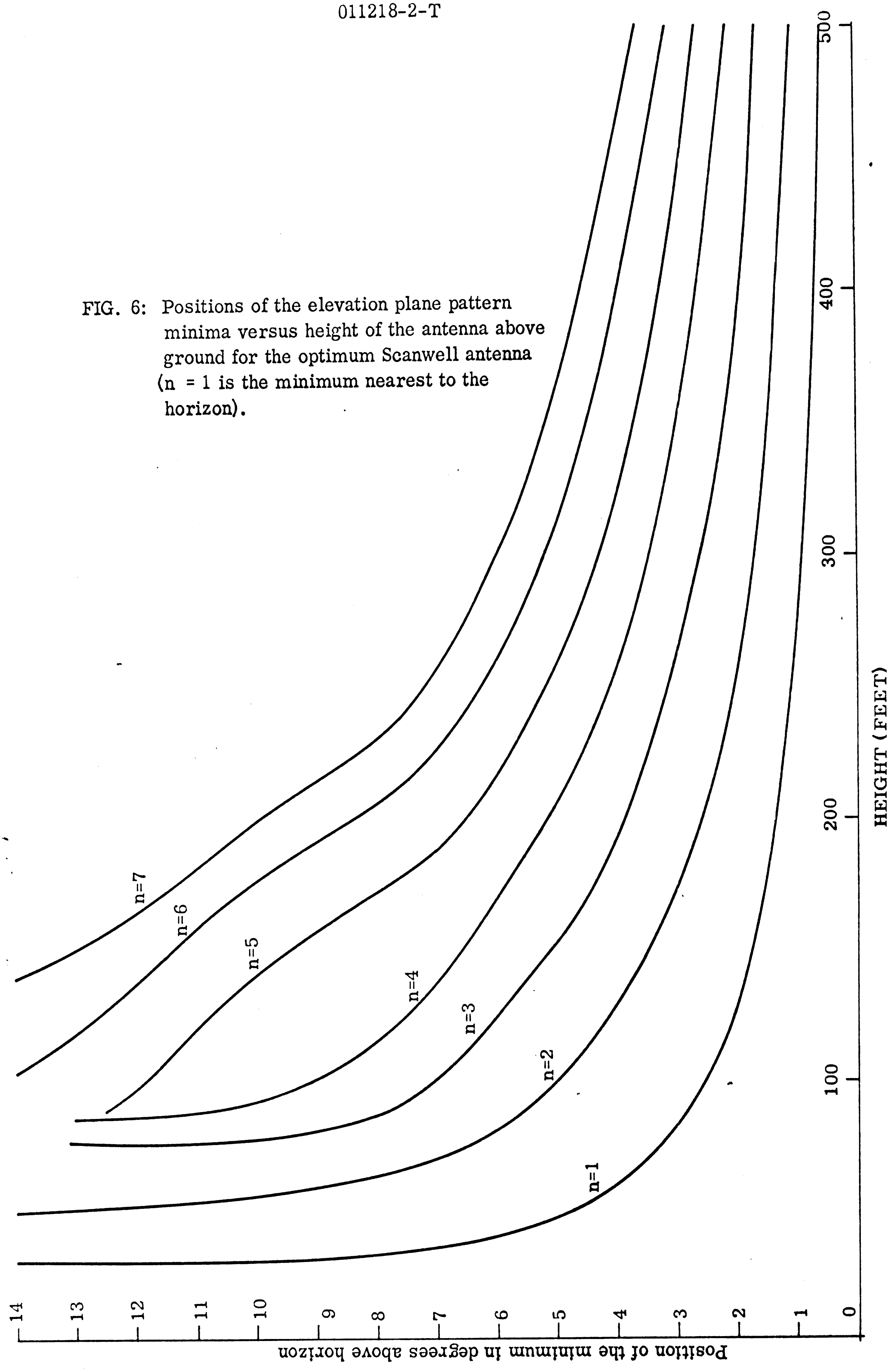

FIG. 6: Positions of the elevation plane pattern minima versus height of the antenna above ground for the optimum Scanwell antenna (n = 1 is the minimum nearest to the horizon).

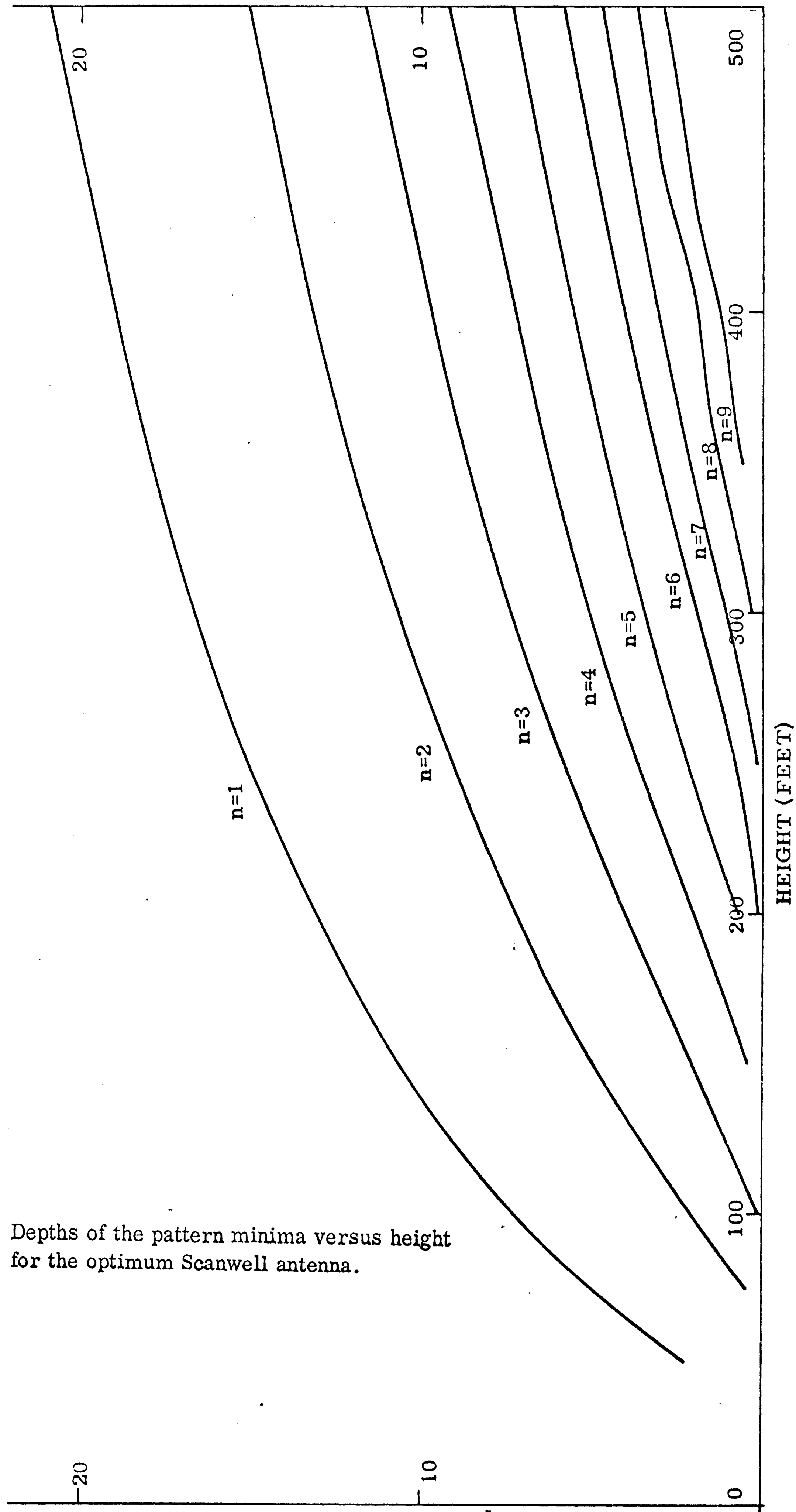

FIG. 7: Depths of the pattern minima versus height for the optimum Scanwell antenna.

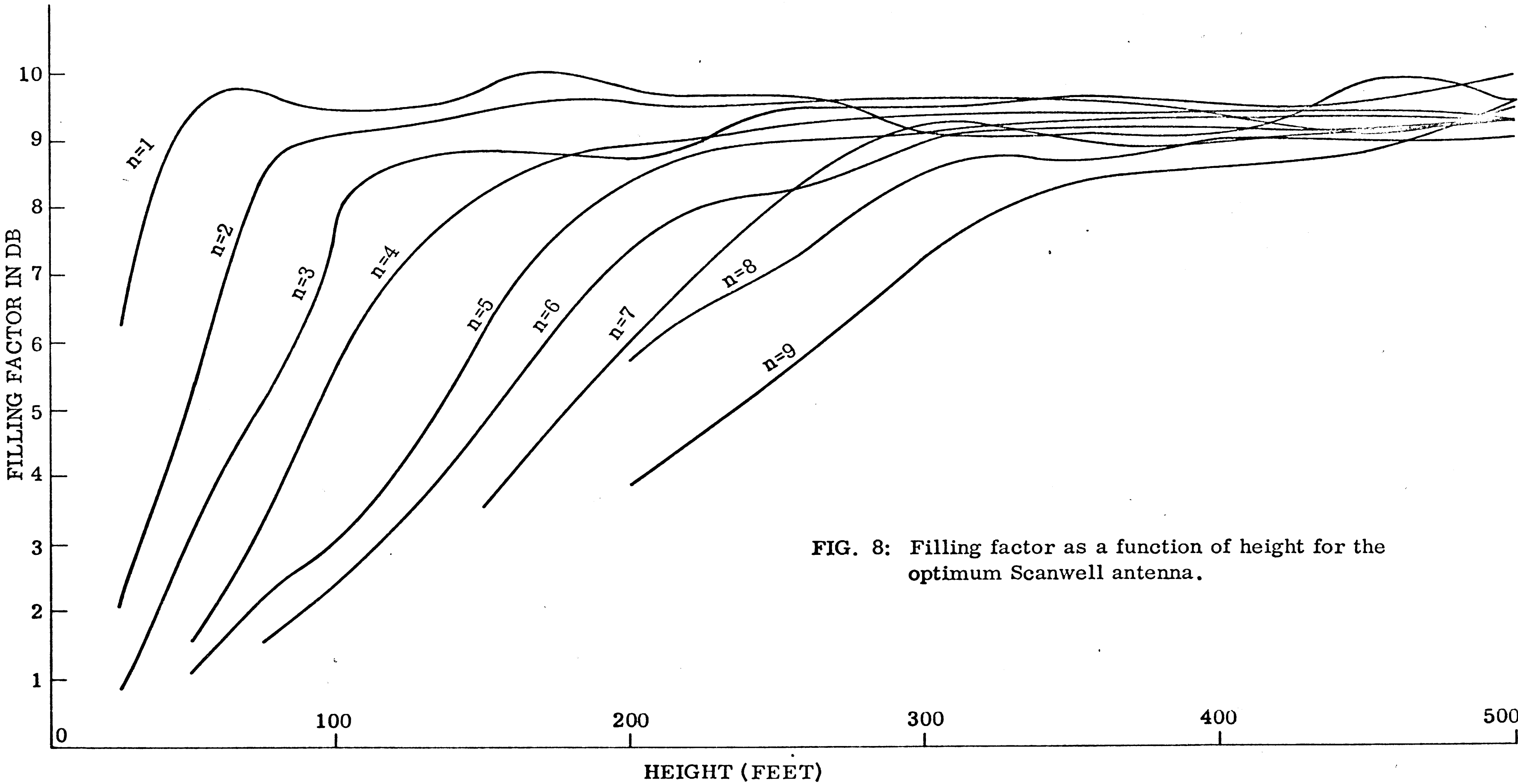

FIG. 8: Filling factor as a function of height for the optimum Scanwell antenna.

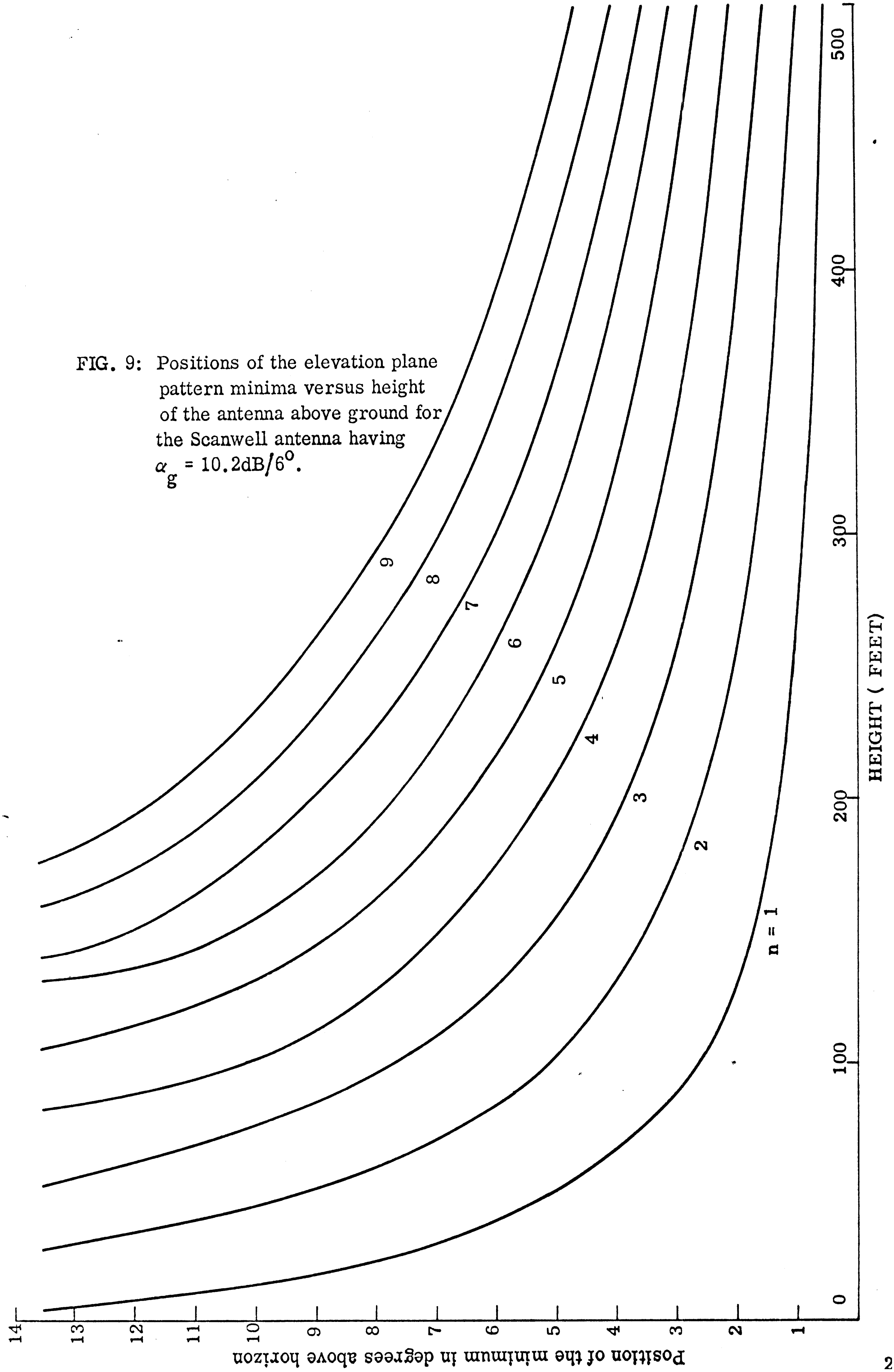

FIG. 9: Positions of the elevation plane pattern minima versus height of the antenna above ground for the Scanwell antenna having $\alpha_g = 10.2\text{dB}/6^{\circ}$.

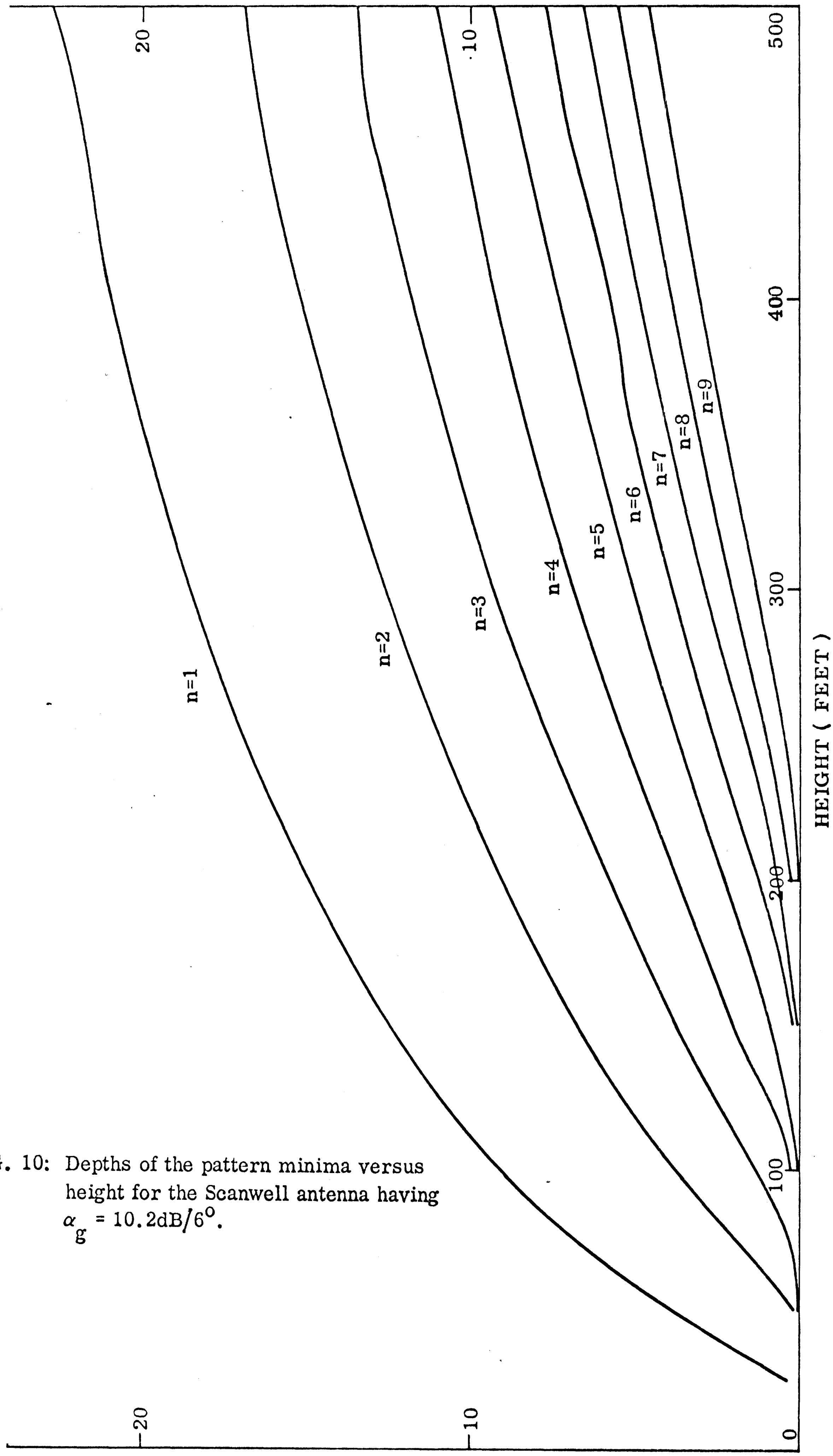

FIG. 10: Depths of the pattern minima versus height for the Scanwell antenna having $\alpha_g = 10.2\text{dB}/6^{\circ}$.

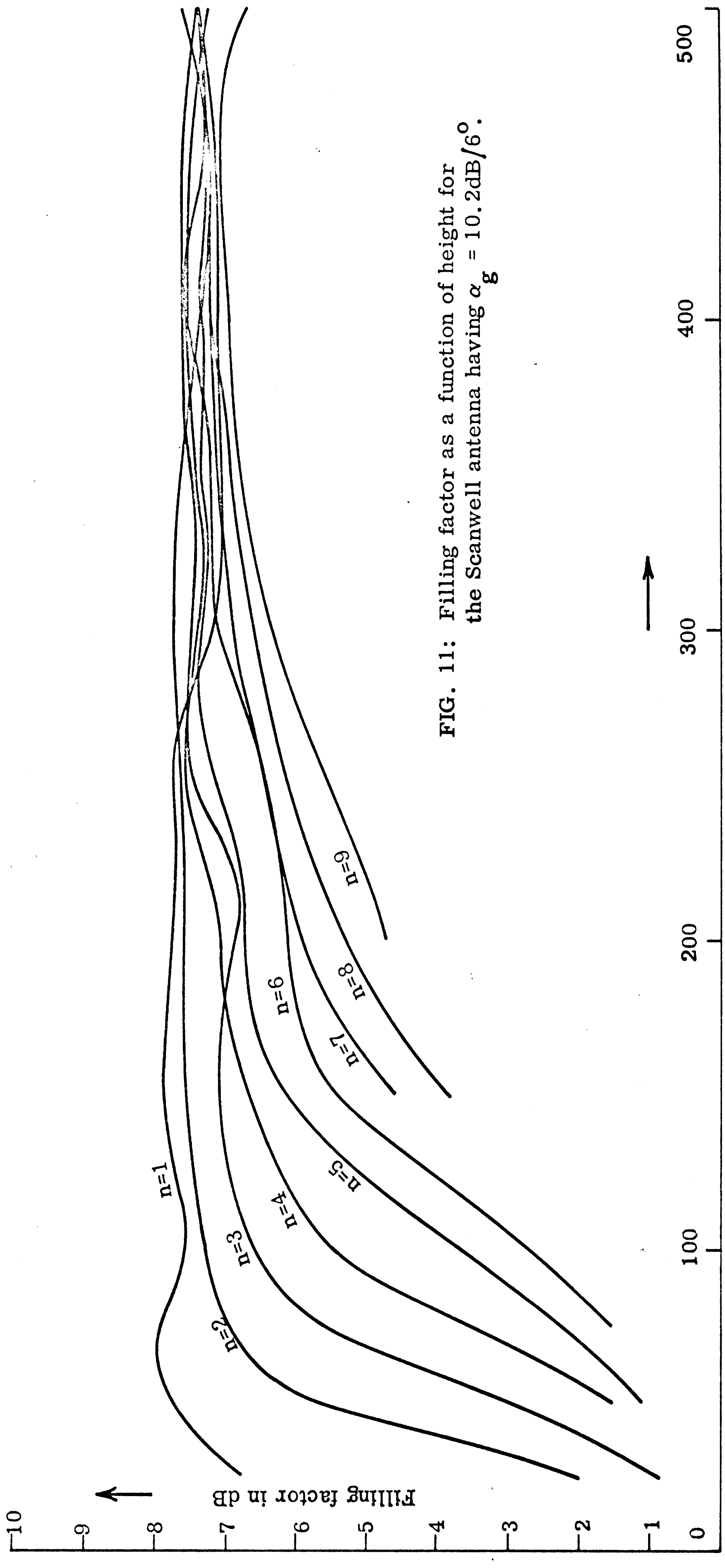

FIG. 11: Filling factor as a function of height for the Scanwell antenna having α_g = 10.2dB/6°.

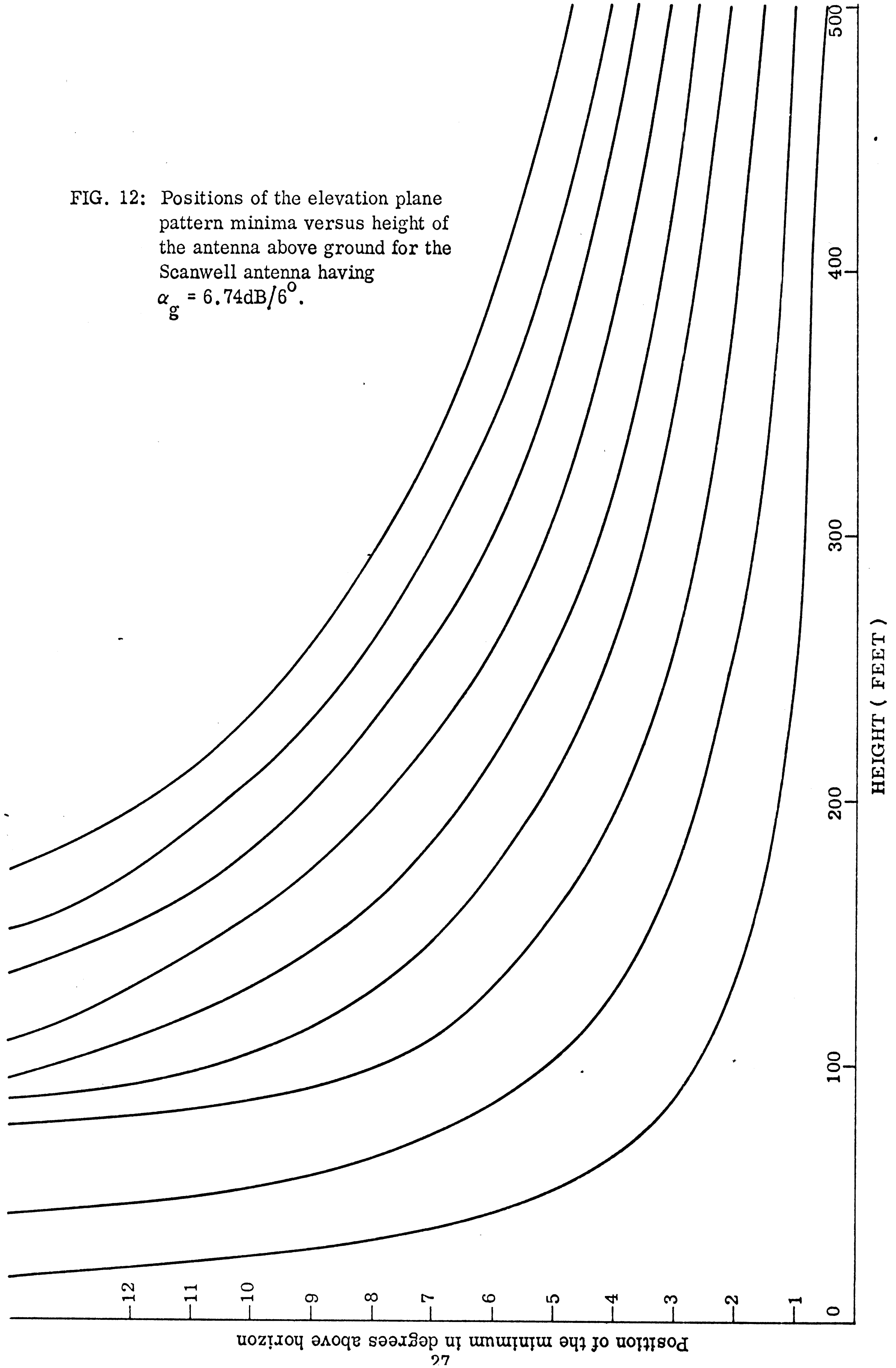

FIG. 12: Positions of the elevation plane pattern minima versus height of the antenna above ground for the Scanwell antenna having $\alpha_g = 6.74\mathrm{dB}/6^{\circ}$.

FIG. 13: Depths of the pattern minima versus height for the Scanwell antenna having $\alpha_g = 6.74 dB/6^o$.

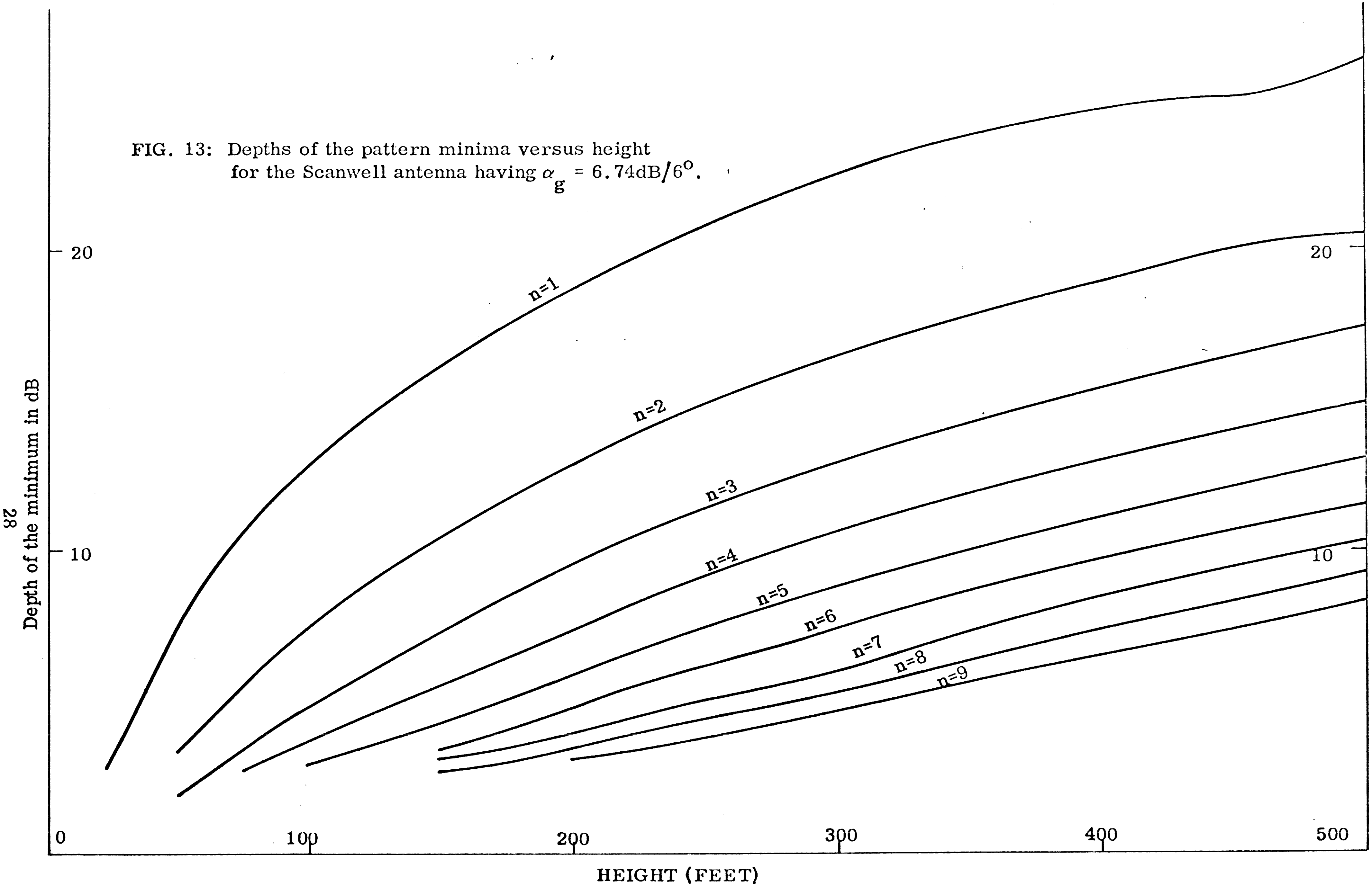

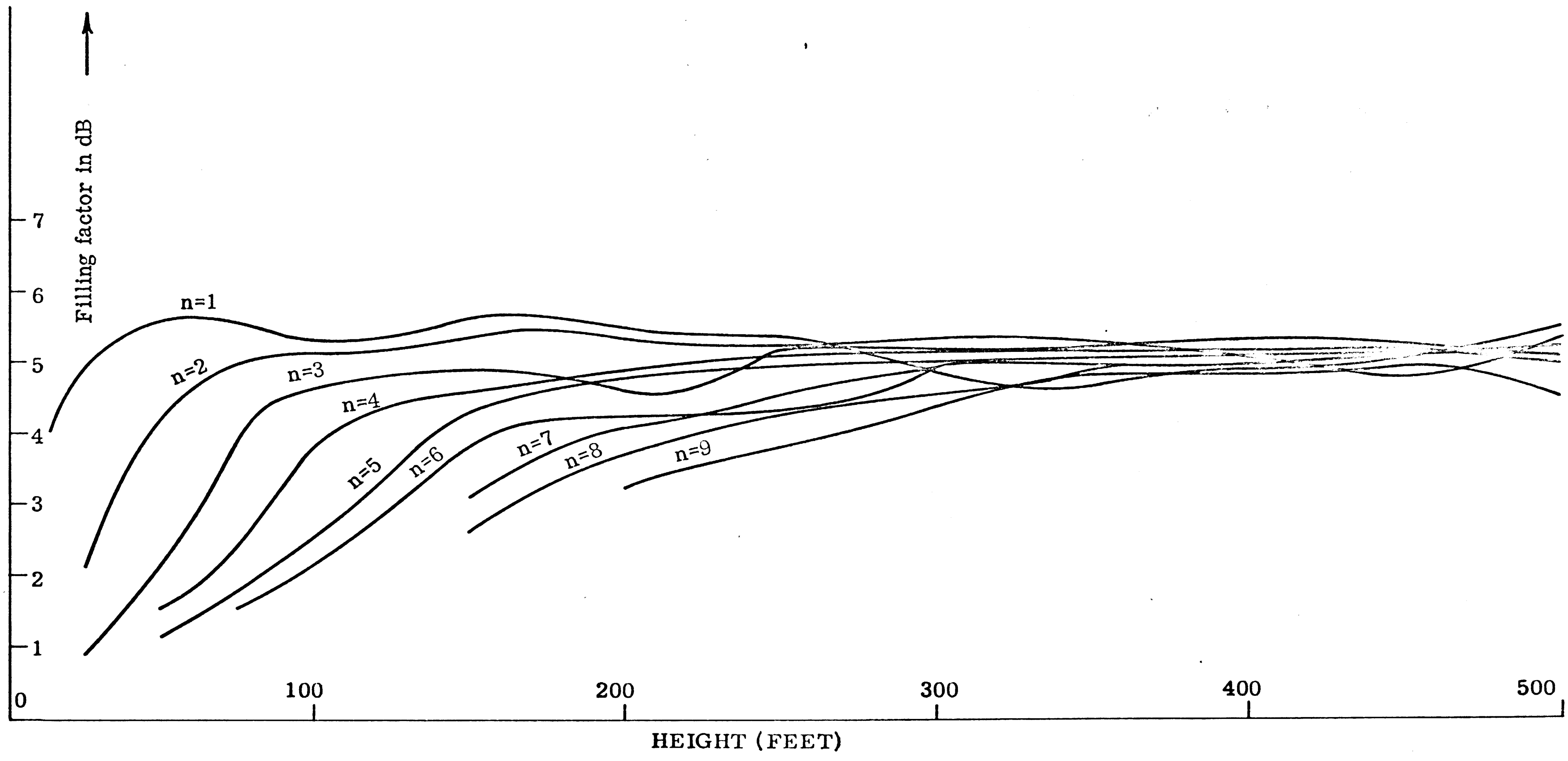

FIG. 14: Filling factor as a function of height for the Scanwell antenna having α_g = 6.74dB/6°.

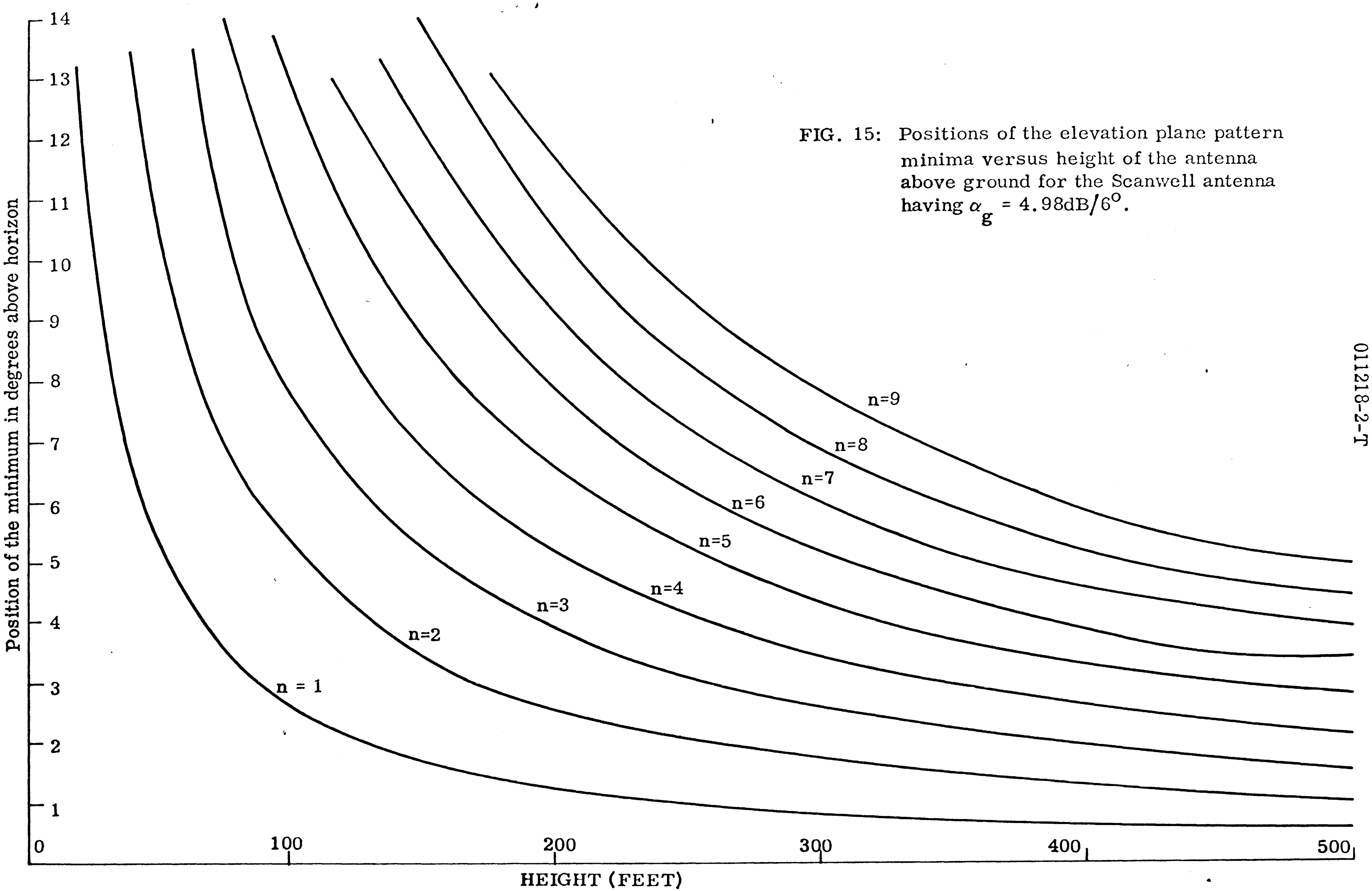

FIG. 15: Positions of the elevation plane pattern minima versus height of the antenna above ground for the Scanwell antenna having $\alpha_g = 4.98 dB/6^o$.

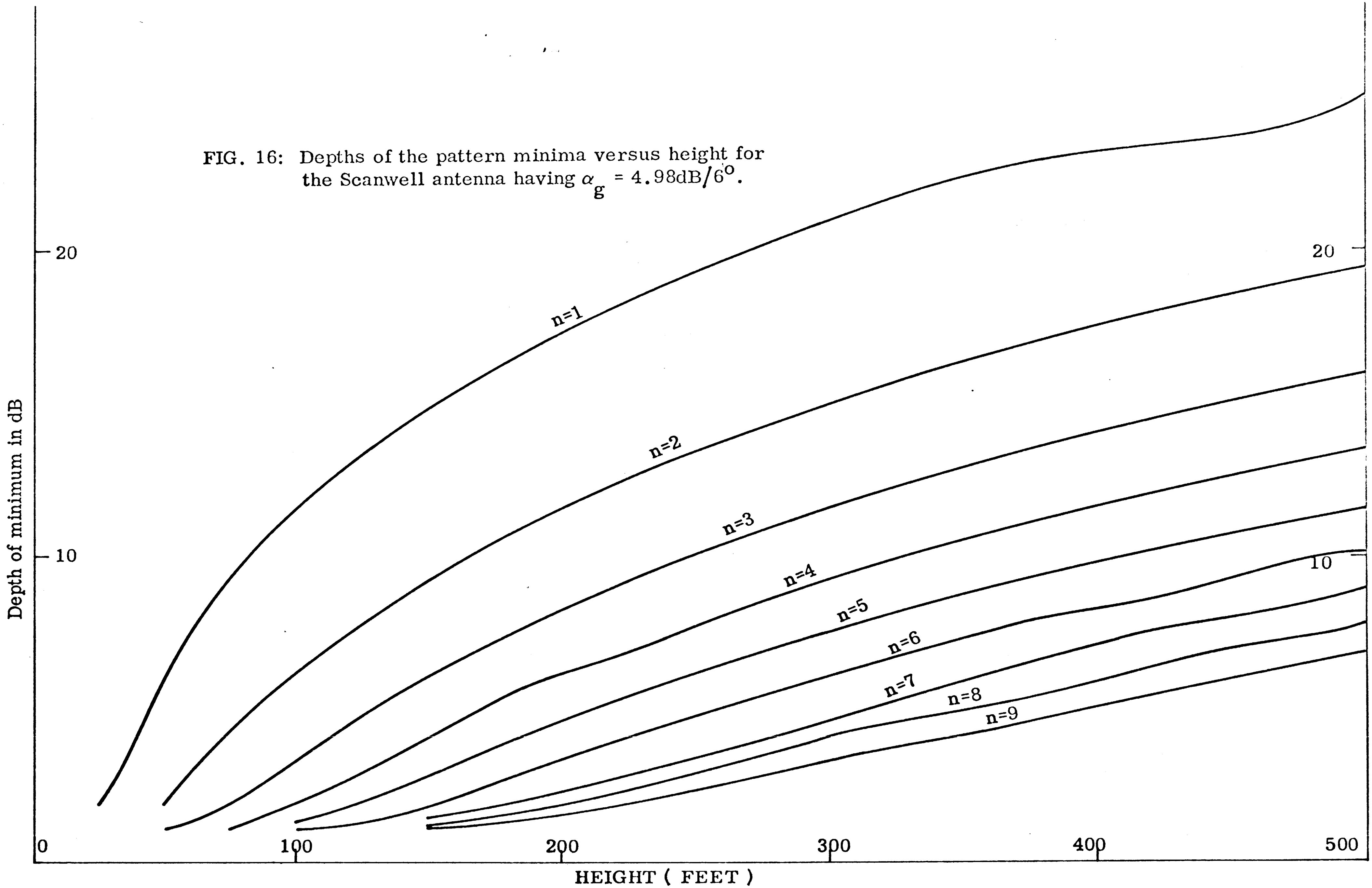

FIG. 16: Depths of the pattern minima versus height for the Scanwell antenna having $\alpha_g = 4.98 dB/6^o$.

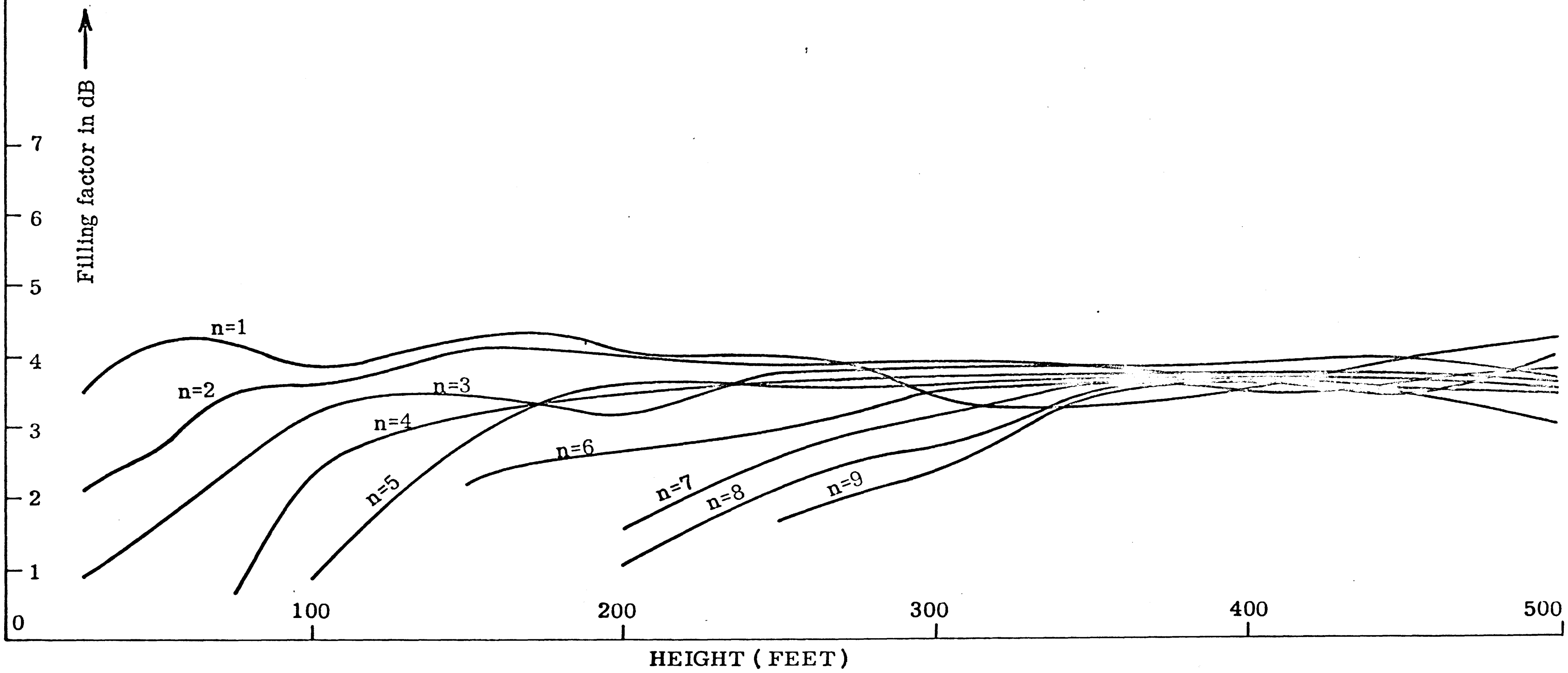

FIG. 17: Filling factor as a function of height for the Scanwell antenna having $\alpha_g = 4.98\text{dB}/6^{\circ}$.

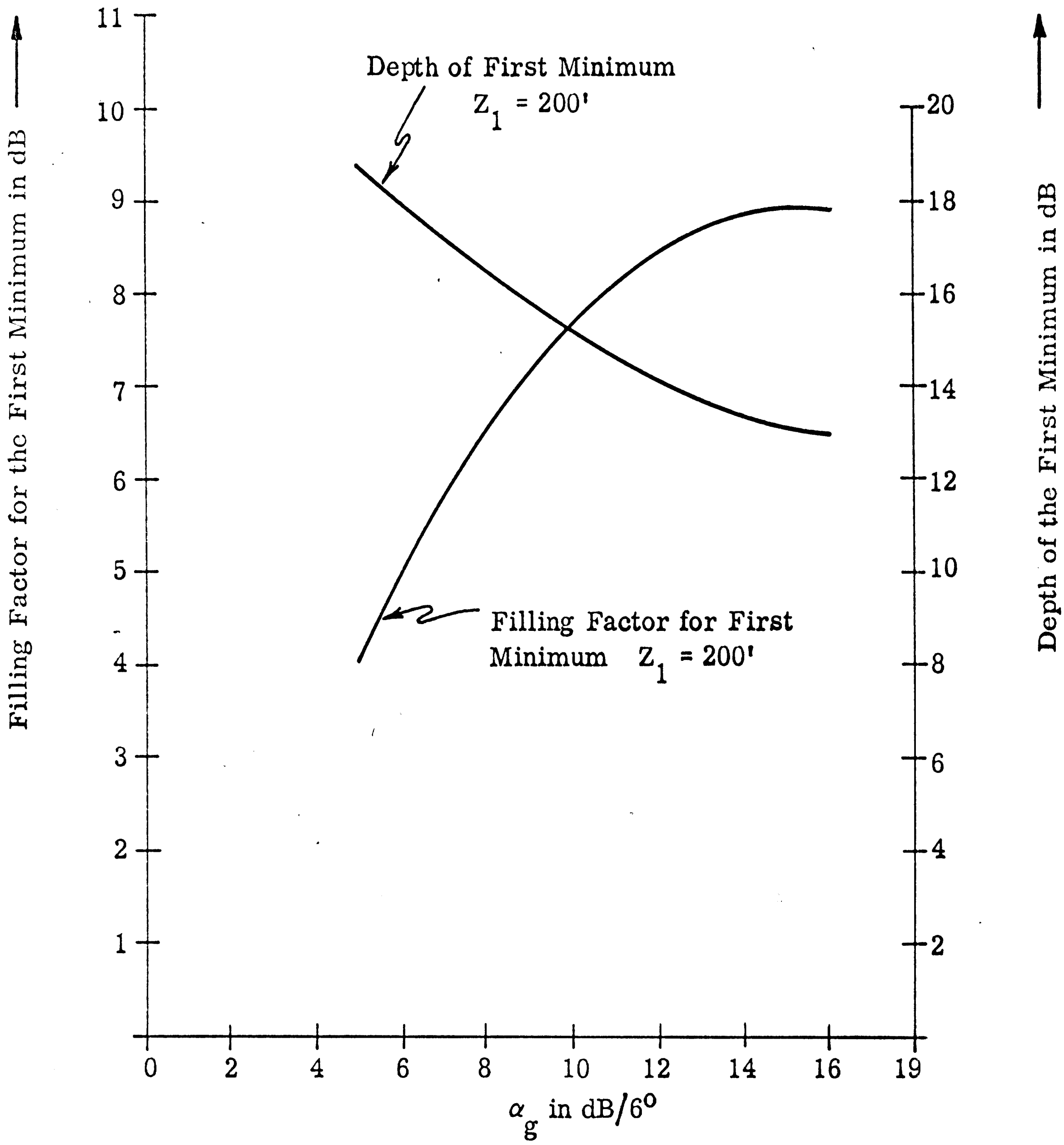

FIG. 18: Depth of the first minimum and the filling factor for the first minimum as functions of the field gradient α_g.

V

REFERENCES

Anderson, S.R., H.F.Keary and W.L.Wright (1953), The Four-Loop VOR Antenna, Technical Development Report No. 210, Civil Aeronautics Administration Technical Evaluation Center, Indianapols, Indiana.

Sengupta, D.L. and P. Chan (1972), Application of the Large Gradient VOR Antenna, Interim Engineering Report No. 1, University of Michigan Radiation Laboratory Report 011218-1-T, Ann Arbor, Michigan.